A Possible Role of Radial Electric Field in Driving Parallel Ion Flow in the Scrape-off Layer of Divertor Tokamaks

A.V.Chankin[1], D.P.Coster[1], N.Asakura[2], G.Corrigan[3], S.K.Erents[3], W.Fundamenski[3], H.W.Müller[1], R.A.Pitts[4], P.C.Stangeby[5], M.Wischmeier[1]

[1] *Max-Planck-Institut für Plasmaphysik, EURATOM Association, 85748 Garching, Germany*
[2] *Japan Atomic Energy Agency (JAEA); Naka Fusion Research Institute, 801-1 Mukouyama, Naka-Machi, Ibaraki-ken, 311-0193, Japan*
[3] *EURATOM-UKAEA Fusion Association, Culham Science Centre, Abingdon, Oxfordshire, OX14 3DB, UK*
[4] *Centre de Recherches en Physique des plasmas, Association EURATOM-Confédération Suisse, École Polytechnique Fédérale de Lausanne, Ch-1015, Switzerland*
[5] *University of Toronto Institute for Aerospace Studies, 4925 Dufferin St., Toronto, M3H 5T6, Canada*

Abstract

The radial electric field in known to be one of the drivers of parallel ion flow in the SOL. It contributes to the ion Pfirsch-Schlüter flow and also determines the 'return parallel flow' that can arise to compensate poloidal E×B drift. It was established recently that 2D fluid codes EDGE2D and SOLPS underestimate the predicted E_r in the SOL compared to experimentally measured values. The underestimate is likely to be related with kinetic effects of parallel transport by heat-carrying electrons. The present work demonstrates that this underestimate can be responsible for the large discrepancy between measured and simulated parallel ion flows in the SOL observed in a number of experiments. Were the radial electric field modelled correctly by the codes, a significant increase in the predicted Mach number of the parallel ion flow could be expected. For the part of the ion flow that depends on the toroidal field direction, this would greatly reduce, or even possibly eliminate, the difference between the experiment and model, as concluded from the comparison between measured and simulated radial electric fields and Mach numbers of the parallel ion flow in JET and ASDEX Upgrade.

1. Introduction

Discrepancies between measured and modelled parallel ion flows in the scrape-off layer (SOL) are one of the unresolved issues in tokamak edge physics. They manifest themselves as repeated failures of the present-day 2D codes to simulate the large flows observed in the 'main SOL', far away (upstream, along field lines) from the divertor region (see e.g. [1,2]). Typically, the two of the most widely used edge codes – EDGE2D and SOLPS, predict parallel ion flows which are considerably below those evaluated experimentally using double-sided Langmuir probes ('Mach probes'). This raises a basic question about our understanding of the key plasma and/or neutral transport mechanisms in the SOL and divertor. The problem is most pronounced on JET, where edge plasma simulations with the EDGE2D plasma code coupled with the Monte-Carlo neutral solver Nimbus produced Mach numbers of the parallel ion flow that were up to an order of magnitude, by factor 5-10, lower than the measured values (typically ~ 0.5) [1]. Such a striking disagreement between the code results and experiment led the authors of [1] to explore the possibility that the high Mach numbers in the experiment are an artifact of the experiment due to impurities generated at the probe by plasma-surface interaction during the measurement itself. Modelling with the SOLPS code package which consists of the B2.5 plasma code coupled with the Monte-Carlo neutral solver Eirene produced a somewhat smaller discrepancy [3], but no direct comparison between SOLPS cases and JET measurements were made. High Mach numbers of the parallel ion flow, close to the JET values, ~ 0.5, were confirmed on ASDEX-Upgrade (AUG) [4,5]. SOLPS modelling however predicts smaller values, roughly by factor 3, as shown below. On JT-60U, measured ion flows were also found to be by factor ~ 2 above those predicted by the UEDGE code [6].

Recently, benchmarking of the SOLPS code against experimental data of AUG has uncovered another problem with the modelling: the tendency of the code to underestimate divertor T_e and overerestimate its density. This was established in well-diagnosed H-mode [7] and Ohmic [8] shots. (In the H-mode modelling, inter-ELM outer midplane n_e and T_e profiles, input power into the grid corrected for the rate of increase in the stored energy in between ELMs, and radiated power corrected for ELMs contributions, were the main input parameters for the code runs, as described in [7]). It was tentatively concluded that the discrepancies between the code and experiment should be attributed to non-local kinetic transport of electrons along the field lines. Such kinetic effects are not covered by the fluid codes. They, however, can be important even in the SOL where the plasma is usually considered to be strongly collisional. Under typical plasma conditions, supra-thermal electrons in the 'main SOL', responsible for the bulk of the parallel electron heat transport to the divertor, with velocities in the range of 3 - 5 of electron thermal velocity $v_{T_e} = \sqrt{T_e / m_e}$ (see [9] and refs. therein, also [10]), appear to be only weakly collisional. Plasma conditions in the main SOL, upstream of the divertor, are typically characterized by the ratio of the Coulomb collisional mean-free path λ to the parallel plasma parameter variation scale length L above 0.01 (from 0.01 for high density Alcator C-Mod plasmas to ≈ 0.2 for low density TdeV and DIII-D plasmas, according to [9]; effective dimensionless electron collisionality, which is close to the inverse ratio, L/λ, is ≈ 15 for the higher density phase of the standard AUG Ohmic shot [2]). λ/L ratios of ≈ 0.2 [9], or, according to the estimate of [2], effective electron collisionality ≈ 12, corresponding to $\lambda/L \approx 0.08$, are expected in ITER. The effective λ/L ratio for heat-carrying electrons, owing to the velocity scaling $\lambda \propto v_e^4$ for the Coulomb mean-free path, is by two orders of magnitude higher than the λ/L ratio for thermal electrons, making heat-carrying electrons only weakly collisional. Typical SOL and divertor conditions with upstream T_e much greater than the downstream value and the upstream λ/L ratio of 0.1 were

modelled with the kinetic Fokker-Planck code [9]. Large distortions of the electron distribution function at the 'cold end', with grossly over-populated high-energy tail (compared to the Maxwellian distribution) were found, leading in particular to enhanced Debye potential drops at the target.

It was hypothesized in [11] that the two problems: failure of today's codes to model fast parallel ion flows in the SOL and their underestimate of divertor T_e, are connected with each other, with the connection between them being provided by radial electric field, E_r, which was found to be larger in the SOL for 'hot' (with high T_e) divertor solutions. The ensuing comparison between measured and modelled profiles of E_r on different machines demonstrated the existence of a large discrepancy between the two, with the codes grossly underestimating E_r in the SOL [12]. Very low E_r were obtained in the SOLPS and EDGE2D modelling, with $-eE_r/\nabla T_e$ ratios close to zero, or, as a maximum, ~ 0.5. In contrast, experimental values of this ratio were ≈ 1.6 for JET, ≈ 3.1 for AUG, ≈ 2.5 for JT-60U and from 3 to 5 for TCV. The formula $e(V_p-V_f)/T_e = 3$ for deriving E_r values was used in [12]. The large discrepancy between the modelling and experiment is thought to arise entirely from deficiencies of the present-day 2D fluid codes. This view is also confirmed by the fact that measured flows were found to be in a good agreement with the calculated ion Prirsch-Schlüter flow when all the inputs into this formula are taken from the experiment itself rather than from the codes [13,14]. The present paper provides an explanation for the discrepancies between measured and modelled ion flows by analysing the role or E_r in driving parallel ion flows in the SOL.

Since the most striking discrepancies between measured and modelled parallel ion flows were reported from JET, it is of prime interest to analyse the data from this machine. On the other hand, up to date JET is the only machine where a thorough systematic study of the problem of parallel ion flows has been carried out. The JET data are complete in containing all relevant experimental information, including T_e, density and electric potential profiles in the SOL for large number of shots covering various configurations (toroidal field B_t, plasma current I_p), plasma densities, and confinement modes (Ohmic, L- and H-modes). Also, a number of real JET plasmas was modelled with EDGE2D in order to explain the measured SOL flows. Regarding experimental information, the focus of this paper will therefore be on JET, but some analysis relevant to other machines, e.g. AUG, JT-60U and TCV will also be provided.

2. Measurements of parallel ion flow in JET

Parallel ion flow in JET is measured by fast reciprocating Langmuir probes. Two probes are used at different toroidal locations, each capable of measuring ion saturation currents, I_{sat}, facing outer and inner divertors along field lines. The poloidal position of the probes is indicated in Fig. 1. Experimental electron temperature, density and plasma electric potential invoked from the probe measurements can be considered representative for the whole 'main SOL', being mainly functions of the flux surface. This however is not true for parallel ion flow that can vary significantly depending on the poloidal angle. The scientifically motivated choice of the poloidal position for the probe (when only one location is used) should be dictated by the requirement of capturing largest contributions to the total ion flow from a number of possible mechanisms, 'drivers' for the parallel flow. They should be strongly dependent on the discharge parameters, enabling one to discern the underlying mechanisms by conducting experiments in different regimes and magnetic configurations. From this viewpoint, the location of the JET probe is beneficial, as it picks up both flows caused by the drifts and by the 'ballooning' of the cross-field transport (see below). For the purposes of this

paper which deals mostly with the contribution from the E×B drift, such a position however is not ideal, and the more advantageous position would be near the outer midplane position, as was the case in experiments on AUG, JT-60U and TCV. This disadvantage, however, is outweighed by the completeness of experimental information supplied from JET experiments.

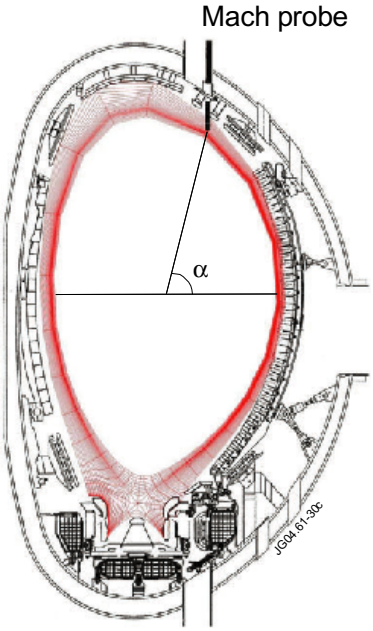

Fig. 1. Poloidal position of reciprocating Langmuir probes in JET.

JET experiments can be performed in two different magnetic configurations: with 'normal' and 'reversed' toroidal field, B_t, directions. In the normal B_t configuration, the ion ∇B drift is directed towards the active divertor which is at the bottom of the machine in the experiments described here. In the reversed B_t configuration, the direction of the ion ∇B drift is reversed. In JET, the direction of the plasma current I_p is reversed simultaneously with the B_t reversal, in order to keep the same helicity of the field lines. To determine the Mach number from the asymmetry of ion saturation currents measured by the two faces of the reciprocating probe ('Mach probe'), Hutchinson's formula $M_{\|} = 0.4 \ln(j_{sato} / j_{sati})$ [15], with j_{sato} and j_{sati} being probe saturation current densities facing outer and inner divertor, was used. Positive Mach numbers, according to JET nomenclature, imply ion flows from the outer to inner target.

Fig. 2 shows measured Mach numbers of the parallel ion flow for JET plasmas in both normal and reversed configurations in a series of Ohmic shots with variable safety factor q_{95} [1], as a function of the distance from separatrix mapped to the outer midplane position. The Mach number, averaged over the two configurations, is shown by the line labeled 'Average'. The average Mach number, which varies roughly between 0.2 and 0.3, corresponds to the ion flow from the outer to inner target. This is usually regarded as a consequence of the ballooning nature of the cross-field particle transport (see below). The part dependent on the B_t direction can be evaluated by subtracting the average Mach number from the locally measured one, or simply by subtracting reversed B_t values from the normal ones. The maximum value thus obtained is $\Delta M_{max} \approx 0.52$. Below, a half of this value, $\Delta M_{max}/2$, which is ≈ 0.26 in this series of shots, will be used as a figure of merit to characterize the effect of the field direction. Density scans were also performed in these experiments, with the line average electron density

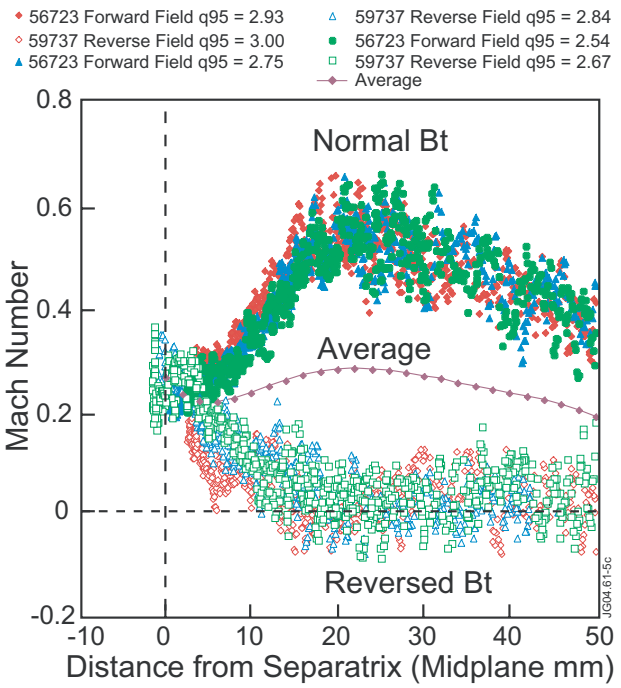

Fig. 2. Mach numbers of parallel ion flow in normal and reversed field (B_t) configurations, in a series of Ohmic shots with variable q_{95}. Figure replicated from ref. [1], with minor alterations.

varying between 1.7×10^{19} and 3.2×10^{19} m^{-3}. At higher densities, $\Delta M_{max}/2$ tended to decrease. Its variation in the series of density scan shots was within 0.25-0.34 [1]. Various other signals and profiles were gathered in these experiments, necessary to characterize the SOL and divertor plasma and to compare the results of the Mach number measurements with models, theories and code simulations. In particular, plasma electric potential (V_p) profiles across the SOL were evaluated from probe floating potential and T_e measurements. They created a large database covering plasmas in different confinement regimes (Ohmic, L- and H-modes). The results and implication of these measurements for the determination of E_r were analysed in the recent paper [12]. They will be used in the analysis of Section 6.

3. Drift flows and flows due to 'ballooning' feature of cross-field transport

As shown in the previous section, the pattern of flows in JET is such that they can be broken down into the two main components: field-dependent, implying the direction of the toroidal field B_t, and field-independent, averaged between the two field configurations (see e.g. review paper [16] and references therein). This separation is justified by the existence of the two dominant mechanisms believed to be responsible for the parallel flow pattern in the 'main SOL', away from the X-point and divertor. One is the consequence of the ballooning nature of the cross-field particle flux, discussed just below, and the other – quasi-steady-state drift motions. The direction of the latter depends on the B_t direction. Average Mach numbers are usually related with the ballooning mechanism, believed not to be affected by the B_t direction, while the difference between Mach numbers in the two field configurations is attributed to the effect of E×B, ∇B and centrifugal drifts. Other processes, namely particle sink to the target and neutral ionization in the SOL and divertor, also contribute to the flow pattern in the 'main SOL', but they are usually considered to be less important on the outboard, low-field side, where ion flow measurements are usually conducted.

To assess the contribution of drift effects to parallel ion flows, which is the main purpose of this paper, one should therefore first subtract the field independent (average between normal and reversed field configurations) flow attributed to the 'ballooning'. This mechanism of cross-field plasma transport was invoked in earlier papers in order to explain various aspects of power and particle flow at the plasma edge. The 'inside-outside asymmetry of particle and energy flow' was mentioned in [17] as an explanation for a much higher, by factor 5, particle and energy flows to the outside SOL than to the inner one in double-null divertor operation in ASDEX and PDX. Later, 'poloidally asymmetric diffusion' favouring outer, low-field side, with $D_\perp$ there exceeding that on the inner side by factor 5-30, was established by using poloidally distributed probe array in Alcator C, which showed large poloidal asymmetries of n_e, T_e and radial density e-folding length in the SOL [18]. A further advance was made with the use of multiple Mach probes introduced at different poloidal locations for measuring parallel ion flow in field reversal experiments aimed at separating drift-related flows from those which are caused by asymmetries in the plasma transport. The term 'ballooning' in relation to poloidally asymmetric transport, was used to describe the results of ion parallel flow measurements in T-10 [19], where it was formulated as 'preferential plasma escape to the external circumference of the torus', and later as 'enhanced particle diffusion at the outside midplane' in DITE experiments [20]. With Mach probes, one can establish the ballooning mechanism by observing its consequence – plasma flow along field lines from the outer to inner part of the flux surface. Parallel plasma flows from the outside to inside of the torus were often characterized by such high Mach numbers that it would require almost all cross-field plasma transport to occur through the outer side [20]. As a concrete mechanism for the generation of large particle flux through the low field side, intermittent blobby-type transport was recently proposed in [21].

It was recently realized, however, that such parallel flows pose a problem of particle sinks. Indeed, such a large parallel flow to the inside of the torus can lead to fast uncontrolled density rise there, unless it is compensated by some mechanism that removes the plasma. Attempts to simulate large Mach numbers of the parallel ion flow at the top of the machine, comparable to those seen in JET experiments, by introducing large asymmetries in particle and/or energy cross-field transport by one of the authors of this paper (AVC) were unsuccessful, with the inner divertor seemingly serving as a baffle, not allowing the (desired large) parallel ion flow to pass further and hence restricting it everywhere else in the SOL. The danger of an uncontrolled density rise was automatically avoided in these EDGE2D code simulations by self-adjustment of the radial density gradient (the separatrix density was fixed), making the cross-field flux $-D_{\perp}\nabla n_e$ consistent with particle sinks at the target/wall and the neutral penetration into the core.

Large parallel flow can however be obtained in the codes if one additionally introduces a pinch term on the inner side of the flux surface, thereby creating a closed loop of the particle circulation in the torus [22], similar to the one arising due to vertical electric field and E×B convection caused by the Pfirsch-Schlüter current, but with a much higher flux densities. No concrete physical mechanism in support of such a pinch has however been offered. An alternative explanation for closing the loop, by neutrals rather than ions, is based on results of UEDGE modelling of DIII-D plasmas, where penetration of recycled neutrals into the core SOL was shown to be strongly poloidally non-uniform, with the bulk of the neutral flux concentrated near the X-point on the inner (high-field) side of the SOL (the X-point was located at the bottom of the machine) [23]. A similar result was obtained in SOLPS modelling of Alcator C-Mod plasmas [24]. This might explain observations of strong, near-sonic parallel ion flows at the high-field side of the SOL in Alcator C-Mod [25]. Accurate description of neutral penetration into the confined region is also important for correct simulation of target temperatures. As was shown in [26], the temperature difference between midplane and target plate and the density near the target are much smaller than in the case when this penetration is not treated properly.

Another possibility for creating a large-scale circulating of particles - via neutrals penetrating from the inner to outer divertor, was predicted by SOLPS (B2-Eirene) simulations of the divertor plasma in ITER [27]. It, however, strongly depends on the divertor geometry and especially on the presence of a baffle between inner and outer divertors.

4. Modelling parallel ion flows and radial electric field with EDGE2D and SOLPS

The selected EDGE2D cases analysed in this section are based on the earlier modelled Ohmic JET cases described in [1]: #56723 for normal and #59737 – for reversed B_t configurations. The results are presented in Fig. 3 (note that different meshes were used for cases with opposite B_t directions; meshes extended into the core region by 5.1 and 4.6 cm for the normal and reversed field cases, respectively, at the outer midplane position). Two density phases of these shots, referred to below as having 'high' and 'low' separatrix density n_s, were modelled in [1] by varying the amount of the gas puff. The separatrix density was varied from 5×10^{18} to 7.7×10^{18} m^{-3}. This is a somewhat narrower range than that of the line average density variation, from 1.7×10^{19} to 3.2×10^{19} m^{-3}, in the experimental measurements of parallel plasma flows described in Section 2. The experimental target profiles, mainly of the n_e and T_e obtained by Langmuir probes, were reasonably well matched in the EDGE2D modelling.

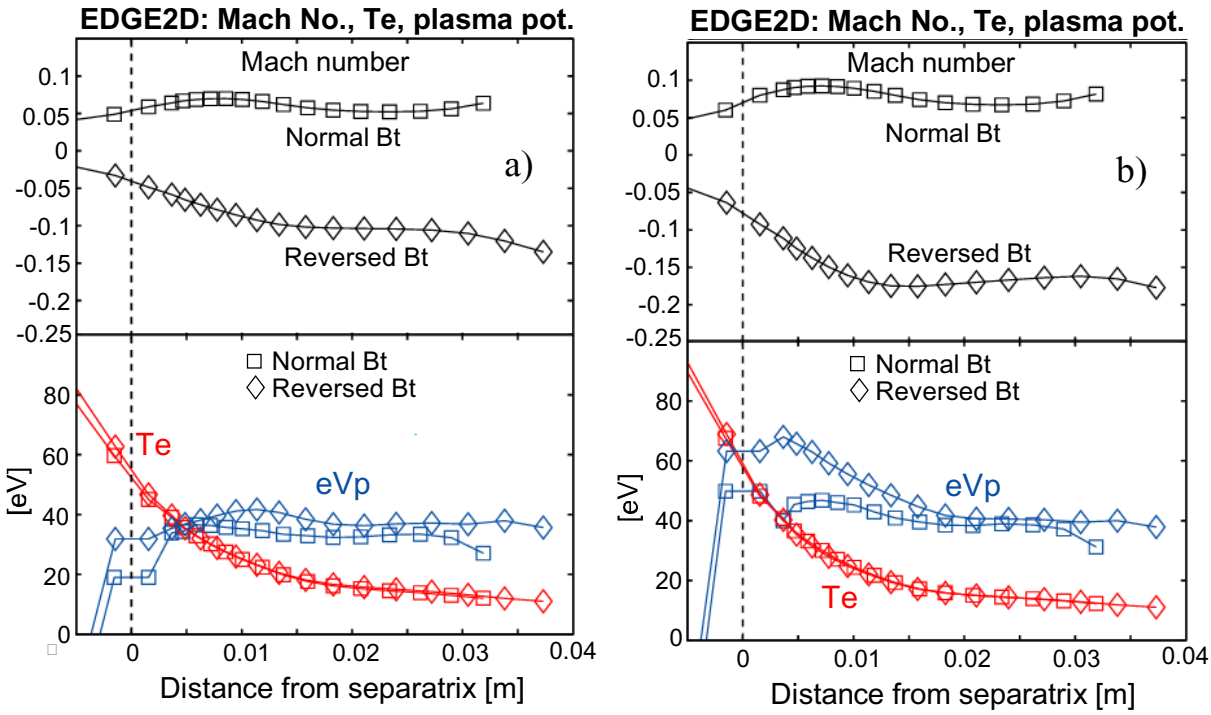

Fig. 3. Mach numbers of the parallel ion flow at the reciprocating probe position, electron temperatures and plasma potentials at the outer midplane position, for Ohmic EDGE2D cases simulating JET plasmas, referred to as having 'high' a) and 'low' b) densities in the text. The distance from the separatrix is mapped to the outer midplane position.

Profiles of midplane T_e and V_p for these Ohmic EDGE2D cases can be found in [12]. The JET H-mode case presented in this ref. has the shape of V_p and values of the Mach number close to those in the high density Ohmic case. In the EDGE2D cases presented here and in [12], drifts were switched on in the whole numerical grid, contrary to earlier modelling described in [1], where due to problems with numerical instabilities drifts where only switched on in the SOL but switched off in the core region. Switching drifts everywhere has not resulted in any significant variation of T_e and V_p profiles in the SOL but considerably affected Mach number profiles: ΔM_{max} increased by factors 1.29 and 1.55 for high and low density Ohmic cases, respectively.

As one can see from Fig. 3, the V_p profiles across most of the SOL show almost no resemblance to the T_e profiles, which is in a striking difference to the experiment where T_e profiles were found to repeat those of the plasma potential, with the ratio $-eE_r/\nabla T_e$ varying between 1.6 and 5. This is one of the reasons why the simulated Mach numbers can be underestimated compared to the experimentally measured values. The 'ballooning' component of the modelled flows, which should result in the average Mach number being positive, cannot be seen in Fig. 3. This is not surprising since poloidally constant transport coefficients were used (but even making the coefficients more 'ballooning' may not have helped to raise significantly the averaged flow, see Section 3). Negative average Mach numbers, increasing with minor radius, can be attributed to the particle sink at the outer target. At larger radii, deeper in the SOL, there is also a tendency for absolute values of the Mach numbers to increase in both normal and reversed B_t cases, which is not observed in the experiment. To characterize the cases, ΔM_{max} will be calculated using Mach numbers from the first 2 cm into the SOL; in this region the peak in the experimental flow is observed. The modelled $\Delta M_{max}/2$ value is 0.08 for the high density and 0.126 – for low density EDGE2D

cases. Mach values for the H-mode case simulated in [28] as well as for the corresponding reversed B_t shot, were close to those for the high density Ohmic case, and the simulated E_r value was around zero in most of the SOL [12].

For comparison, two Ohmic SOLPS cases, simulating AUG plasmas, for high and low separatrix density n_s (which was fixed in the modelling) are presented in Fig. 4. The computational mesh extended into the core region by 8.2 cm, at the outer midplane position. The T_e and V_p profiles were analysed earlier in [12]. Only the normal field case at high n_s represents the simulation of a real AUG plasma, with the other three cases having no experimental analogues. The direction of the positive ion flow/velocity was reversed compared to conventions used in the SOLPS code (where positive direction implies motion from the inner to outer target) to ease the comparison with the EDGE2D cases.

In the SOLPS cases presented in Fig. 4, small anomalous radial currents related to E_r and ∇T_e are used. The anomalous conductivity is controlled by the parameter *fsig*, and anomalous thermo-electric current – by *falf*. The electrical conductivity and thermo-electric coefficients are given by $fsig \times 1.6\times10^{-19} n_e(m^{-3})$ and $falf \times n_e(m^{-3})T_e(eV)^{-1/2}$ is MKS units, respectively. The default values for both parameters, also used in the cases presented here, are 1×10^{-3}. These anomalous currents were introduced into SOLPS for the sake of improving numerical stability of the code. Comparison between selected SOLPS cases with and without these currents (obtained by drastically reducing values of *fsig* and *falf*, down to zero) shows that they can influence code solutions mainly by reducing electric potential on the first ring

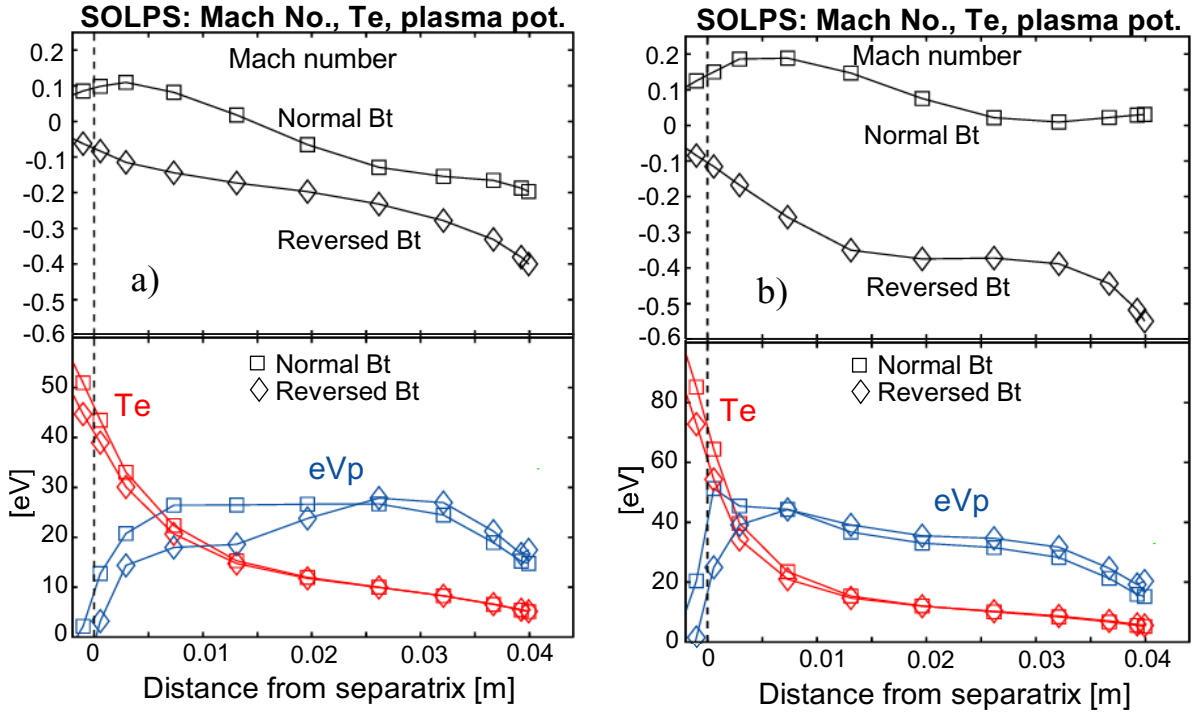

Fig. 4. Mach numbers of the parallel ion flow, electron temperatures and plasma potentials at the outer midplane position, for Ohmic SOLPS cases simulating AUG plasmas, referred to as having 'high' a) and 'low' b) densities in the text.

outside of the separatrix. In the rest of the SOL, E_r is reduced only insignificantly. In contrast, the EDGE2D cases have no such anomalous currents.

Within the first 1 cm into the SOL, corresponding to the region of maximum experimental Mach number (see Fig. 4), $\Delta M_{max}/2$ value increases from 0.114 to 0.241 from high to lower density case. Even the value for the low density case is substantially, by factor 2, below typical experimental values for the Mach number measured in AUG for normal field direction [4]. For the standard Ohmic shot simulated by SOLPS, the maximum experimental Mach number is ≈ 0.45 [4]. The probe in the AUG experiments was introduced from the low-field side, close to the outer midplane position (20 cm above it, with the active divertor located at the bottom of the machine; minor radius was 46 cm), the ion flow should not be strongly affected by the 'ballooning', and one expects approximately the same Much number also for the reversed B_t configuration, but with the opposite sign. One can therefore directly compare the experimental value of M ≈ 0.45 with the modelled $\Delta M_{max}/2 = 0.114$, resulting in the discrepancy between the two values of about factor 4. A possible contribution of the flow caused by the ballooning of the perpendicular transport (owing to the vertically shifted position of the probe with respect to the midplane; this would drive the parallel ion flow in the same direction as measured by the probe) is likely to put a downward correction to this value. The extent of the correction is however difficult to quantify.

Low $-eE_r/\nabla T_e$ ratios following from code runs may raise questions of whether all mechanisms influencing radial electric field in the SOL have been properly incorporated in the codes. Contributions to the E_r coming from terms entering the parallel electron force balance equation, radial non-ambipolarity of the plasma transport, poloidal asymmetries of plasma potential distribution, electric currents flowing to the target, etc., are currently being investigated. For typical plasma edge conditions characterized by not very low densities, low $-eE_r/\nabla T_e$ ratios seem to mainly reflect much lower T_e values at the target than at the outer midplane, as well as fairly flat target T_e profiles. Via the mechanism of the Debye sheath formation, this results in fairly flat upstream plasma potential profiles. At very low densities the codes predict positive outer midplane E_r. However, $-eE_r/\nabla T_e$ ratios are still low, typically not exceeding unity, despite peaking of target T_e profiles. In such conditions, contributions to the parallel force balance equation for electrons, influenced by the 2D ionization pattern in the divertor, may become important in containing the rise of the upstream E_r.

The large, order of magnitude difference between simulated and experimental Mach numbers reported in [1], is an accumulated effect of a few separate contributions from both modelling and experiment. Firstly, most of the attention in this ref. was paid to very large Mach numbers measured in normal B_t configurations. These plasmas are apparently affected by strong 'ballooning', which is characterized by the Mach number ~ 0.2-0.3. The problem of correct modelling of this contribution should be solved by combining strong ballooning of the cross-field transport with more realistic assumptions about particle sources and sinks, work on which is currently underway. Note, however, that modelling the contribution of order 0.2-0.3 is easier than aiming at modelling the whole ~ 0.5 Mach number observed in JET using the ballooning mechanism alone. Large part of the disagreement lies in the failure of the codes to model drift-related flows. These, however, are characterized by smaller Mach numbers, ~ 0.3, than the experimental values for normal B_t plasmas (~ 0.5).

Secondly, as was already mentioned in this section, old EDGE2D cases were run with drifts switched on only in the SOL. This aggravated the comparison with experimentally measured flows by reducing simulated Mach numbers by factors 1.3 – 1.5.

Thirdly, measured E_r in the SOL, as was shown in [12], are significantly larger than the code values, resulting in a much stronger contribution to the ion flow from the E×B drift than calculated in the codes.

Finally, the relative contribution of E_r to the predicted ion flow is likely to be even larger compared to what follows from the Pfirsch-Schlüter formula, due to the existence of the 'return parallel flow' considered in the next section.

The first two contributions alone significantly reduce the difference between modelled and experimental Mach values. Whereas experimental $\Delta M_{max}/2$ values lie in the range of 0.25 to 0.34, the modelling described here gives $\Delta M_{max}/2$ from 0.08 to 0.126. This is roughly a factor of 3 difference. It will be shown below that such a discrepancy can be explained by the code's large underestimate of E_r in the SOL and by the use of more refined formulas for the parallel ion flow velocity. Since realistic code solutions, correctly describing SOL and divertor, are not yet available, one can only project analysis of the existing solutions onto the situation with the increased E_r that is consistent with experiment.

5. Pfirsch-Schlüter flow and 'return parallel flow' compensating poloidal E×B drift

The term 'Pfirsch-Schlüter flow' in relation to the parallel ion flow caused by spatial divergence of perpendicular (within the flux surface but perpendicular to the magnetic field; due to the very small angle between the perpendicular and poloidal directions, the term 'poloidal' will often be used below where it can only result in a small numerical difference) E×B and ion diamagnetic flows in the 'main SOL' was first used by Hugill [29]. The expression for the parallel ion velocity was derived similarly to the derivation of the famous Pfirsch-Schlüter current, by expanding particle balance equation for ions in inverse aspect ratio $\varepsilon = a/R$ and retaining only linear terms. For cylindrical geometry with concentric magnetic surfaces one can easily obtain [29]:

$$V_{i\|PS} = 2\cos\alpha \frac{a}{R}\frac{B}{B_\theta}\left(\frac{E_r}{B} - \frac{\nabla p_i}{enB}\right), \qquad (1)$$

where angle α is counted from the midplane, as shown in Fig. 1, but for cylindrical geometry, and $\nabla p_i \equiv \partial p_i / \partial r$. Ion Pfirsch-Schlüter flow represents the most robust effect of classical drifts in the SOL and is frequently used for comparison with experimentally measured flows. Since this flow peaks at the midplane position, its contribution is easiest to measure when the Mach probe is also positioned at the midplane. Measured parallel ion flows were found to be in good agreement with the Pfirsch-Schlüter formula on JT-60U [13] and TCV [14], where probes were positioned near the outer midplane. The good agreement was achieved eventhough the simpe formula Eq. (1) for cylindrical geometry was used despite the strongly shaped plasmas of the experiments. There is however a number of unknowns in experiments. Indeed, the flow Eq. (1) depends on the ion pressure gradient, and one typically makes an assumption of either $T_i = T_e$ or $T_i = 2T_e$, whereas in reality ion temperature in the SOL is rarely measured. Knowledge of the T_e/T_i ratio is also important to correctly determine the ion sound speed $c_s = \sqrt{(T_e + T_i)/m_i}$ which is used to calculate Mach numbers. The accuracy of Hutchinson's formula for the Mach number of the parallel ion flow, and evaluation of the radial electric field E_r from the floating potential measurements and theoretical expressions for the Debye sheath, also introduce some uncertainty in the comparison between measurements and Eq. (1). SOL flows are also influenced by the particle sink at the target and the ionization source. The agreement of experimental flows with the simple Pfirsch-Schlüter formula, obtained at only one poloidal location, should therefore be

considered as approximate. An extention of Eq. (1) for the case of elliptical geometry is straightforward, resulting in (see Appendix A, Eq. (A10)):

$$V_{i\|PS} = 2\frac{a}{R}\frac{B}{B_\theta}\left(\frac{E_r}{B} - \frac{\nabla p_i}{enB}\right)\left(1+\frac{\tan^2\alpha}{k^2}\right)^{-1/2}, \tag{2}$$

with k being ellipticity $k = b/a$ and angle α counted as shown in Fig. 1. For cylindrical configuration, k = 1, and the angular dependence on the right hand side (RHS) of this equation is reduced to $\cos\alpha$.

The ion Pfirsch-Schlüter flow is not the only effect to be expected from drifts in the SOL. The 'return parallel flow' compensating poloidal (or perpendicular, see just above) E×B drift was theoretically predicted [30] and later found in the output of EDGE2D [31] and SOLPS [32] codes. It was also demonstrated in biasing experiments on TdeV that in response to the applied radial electric field, the SOL plasma changed its toroidal, rather than poloidal, rotation [33]. The velocity of the 'return parallel flow' is, or *may* be (see below) given by:

$$V_{i\|R} = \frac{E_r}{B_\theta}. \tag{3}$$

This flow has the same direction as the Pfirsch-Schlüter flow at the outer midplane, but opposite direction to it - at the inner midplane. At the outer midplane position, the velocity Eq. (3) can numerically be very close to the Pfirsch-Schlüter velocity. The two velocities can therefore be easily confused with each other when measurements are performed only at the outer midplane. For measurements on the inner (high-field) side of the torus, on the other hand, the situation is more complex, since the two flows subtract from each other. In JT-60U experiments in normal B_t direction, the ion flow measured by the Mach probe introduced from the inner (high-field) side above the X-point was directed towards the inner divertor for most of the SOL, against the expected direction of the Pfirsch-Schlüter flow [6]. One always has to remember however that any such comparison can also be affected by the particle sink to the target which was also against the Pfirsch-Schlüter flow on the inner side of the torus in these experiments.

The combined effect of the driving mechanisms given by Eqs. (2) and (3) cannot, however, be represented as a sum of the two velocities. Indeed, the poloidal projection of the 'return parallel flow' Eq. (3), which is obtained by multiplying it by the field pitch angle B_θ/B, already completely compensates for the effect of (mainly poloidal) E×B drift, including both its surface-average and poloidally variable parts. There is no need therefore to retain the part related to E_r in the combined flow as it appears in Eqs. (1,2). The strict derivation is given in Appendix A, resulting in:

$$V_{i\|comb} = \frac{E_r}{B_\theta} - 2\frac{a}{R}\frac{B}{B_\theta}\frac{\nabla p_i}{enB}\left(1+\frac{\tan^2\alpha}{k^2}\right)^{-1/2}. \tag{4}$$

At the midplane, for $\theta = 0, \pi$, the effect of ellipticity disappears, and Eq. (4) is simplified:

$$V_{i\|MPcomb} = \frac{E_r}{B_\theta} \pm 2\frac{a}{R}\frac{B}{B_\theta}\frac{\nabla p_i}{enB}, \quad (5)$$

where the sign '-' is for the outer and '+' for inner midplane positions. At the outer midplane, the numerical difference with the Pfirsch-Schlüter expression is very small, since $2a/R$ is typically ≈ 2/3 for most of the machines. The use of the Pfirsch-Schlüter formula to compare with experimentally measured flows would therefore be almost as good as the use of the formula for the combined flow, if flow measurements were only performed at the outer midplane position.

For positions shifted away from the midplane, on the other hand, such as in the case of the flow measurements in JET, there is a clear numerical difference between Eqs. (2) and (4). Nearer the top of the machine, the 'return parallel flow' becomes the dominant mechanism that can influence the part of the measured ion flow related to the B_t direction. For the JET probe position, taking k = 1.7 and α = 76°, the poloidally variable pressure gradient part of Eq. (4) is multiplied by factor 0.39, and its contribution to the ion flow is reduced accordingly. Hence, the relative role of the 'return parallel flow', which is poloidally constant, increases. The angular dependence in Eq. (4) should of course be considered as very approximate, since, apart from ellipticity, the real plasma shape is also characterized by triangularity and higher shaping moments. In the estimates made for the comparison of the measured flow with the Pfirsch-Schlüter formula in [34], ellipticity was completely ignored, but the angle was chosen to be 60°. The cosine of this angle, 0.5, coincidentally, provided very similar factor of reduction of the Pfirsch-Schlüter velocity to the example considered above.

There is one issue with the inclusion of the 'return parallel flow' in the model that needs to be pointed out. Despite the fact that it has been identified in the codes, the degree of confidence in its magnitude is less than that in the Pfirsch-Schlüter flow. It cannot be ruled out that this flow may be either smaller than given by Eq. (3), or larger than it, depending on the divertor conditions. This is because this flow is not *necessarily* reduced to zero near the X-point, and is therefore dependent on the boundary conditions for particle fluxes at the entrances to both inner and outer divertors. They can be affected by drifts and/or neutral particle ionization in the divertor. For this reason, in the next section, estimates reflecting the factor of increase in the predicted ion flow by the inclusion of more realistic E_r values in the SOL than those coming from the fluid codes, will be made using both formulas (2) and (4).

6. Possible enhancement of modelled parallel flows by realistic E_r

Profiles of the modelled plasma potential presented in Section 4, as well as those obtained for H-mode cases presented in [12], are fairly flat in most of the SOL. Near the separatrix, plasma potential may rise with minor radius, resulting in a negative $E_r \equiv -\nabla V_p$. In low density cases, E_r is small but positive in the outer SOL. As a statistical average, given the variety of plasma conditions in which experiments aimed at measuring ion flows with reciprocating Langmuir probes are carried out, one can take zero E_r to characterize EDGE2D and SOLPS solutions, averaged over the whole SOL. This contrasts with rather steep experimental V_p profiles. As pointed out in the Introduction, the ratio $-eE_r/\nabla T_e$ in experiment is > 1.5, and may rise up to 5 in some cases [12]. Had such large values of E_r been found in the codes, one would have expected modelled parallel ion flows to be substantially larger than presently obtained. The main purpose of this section is to estimate the factor of increase in the flows

that the realistic E_r would provide. Radial electric field will be expressed via electron temperature gradient as $E_r = - f\nabla T_e/e$, with factors $f = 1.6$ for JET and 3.1 for AUG used for numerical estimates, consistent with the experimental results presented in [12] (for the AUG case, the chosen factor f represents an averaged value between individual values obtained from the two pins of the probe, facing outer and inner targets along the field lines). The ratio of the part of the ion flow driven by E_r to that of ∇p_i: $R = V_{i\|\_E_r} / V_{i\|\_\nabla p_i}$, will characterize the factor of increase in the predicted parallel ion velocity (1+R). .

Ratio R depends on particular assumptions made about the nature of the parallel ion flow and on a poloidal location used for the probe measurements. Below, two formulas, for the Pfirsch-Schlüter velocity, Eq. (2), and for the combined flow velocity, Eq. (4), will be used, for the two poloidal locations: at the outer midplane and at the location of the JET reciprocating probe. For the Pfirsch-Schlüter formula, the ratio R can be expressed as:

$$R_{PS} = -\frac{enE_r}{\nabla p_i} = \frac{fT_e}{T_i}\frac{\lambda_{p_i}}{\lambda_{T_e}}, \tag{6}$$

where the decay lengths (e-folding lengths) are used for ion pressure and electron temperature. This ratio is independent of a poloidal position and is not affected by ellipticity. For the combined flow, the ratio is given by:

$$R_{comb} = \frac{fR}{2a}\frac{T_e}{T_i}\left(1+\frac{\tan^2\alpha}{k^2}\right)^{1/2}\frac{\lambda_{p_i}}{\lambda_{T_e}}. \tag{7}$$

For numerical estimates, in addition to the choice of $k = 1.7$ (JET case), $\alpha = 76°$ for the JET probe position and $f = 1.6$, ratios $T_e/T_i = 0.5$ (supported by JET data [1]) and $R/a = 3$, similar on JET and AUG, will be used. The ratio of decay lengths $\lambda_{p_i} / \lambda_{T_e}$ is the most difficult parameter to estimate, since well resolved measurements of ion temperature profiles in the SOL are scares. Good edge T_i profiles are however available for the two AUG shots used recently for detailed comparison between SOLPS modelling and experiment described in [7] for an ELMy H-mode shot and [8] for the standard Ohmic shot. The simulated SOLPS profiles at midplane fitted very well the experimental profiles of n_e, T_e, and T_i. The decay lengths from the simulated profiles at two positions, displaced by 0.5 and 1 cm from the separatrix into the SOL are assembled in Table 1. Average values for the decay lengths from this table are: $\lambda_{Te} = 1.14$ cm, $\lambda_{Ti} = 2.15$ cm, $\lambda_n = 1.62$ cm. They are quite close to those in the Ohmic shot only, where the decay lengths are relatively unchanged across the SOL, whereas in the H-mode shot they are strongly affected by the transport barrier closer to the separatrix, which makes the profiles there sharper than further out in the SOL. For the selected individual decay lengths the relation $\frac{\lambda_{p_i}}{\lambda_{T_e}} = \frac{\lambda_{T_i}}{\lambda_{T_e}}\left(1+\frac{\lambda_{T_i}}{\lambda_n}\right)^{-1}$ gives $\lambda_{p_i} / \lambda_{T_e} = 0.81$. This ratio will be used in the estimates below.

SOLPS case, AUG	Δr (cm)	λ_{Te} (cm)	λ_{Ti} (cm)	λ_n (cm)
Ohmic,	0.5	0.93	2.24	1.51

# 18737	1.0	1.24	1.97	1.64
H-mode,	0.5	0.77	1.44	1.22
# 17151	1.0	1.62	2.96	2.12

Table 1. Decay lengths of electron and ion temperatures, and electron density at the outer midplane position, from the simulated SOLPS profiles at two radial positions, displaced by 0.5 and 1 cm from the separatrix into the SOL, for the two AUG shots. The simulated profiles are in a good agreement with experimental points.

For the Pfirsch-Schlüter flow, the ratio R of the E_r flow drive to that of ∇p_i is given by Eq. (6), resulting in a poloidally constant values 0.649 and 1.257 for factors $f = 1.6$ and 3.1, respectively. Hence, owing to the realistic E_r, one could expect a factor 1.6 or 2.3 increase in the predicted Mach number, depending on the chosen value of f (assuming a value of $R = 0$ as reference).

For the case of the combined flow, ratios R are higher. For the midplane position ($\alpha = 0$) $R_{comb} = \frac{fR}{2a}\frac{T_e}{T_i}\frac{\lambda_{p_i}}{\lambda_{T_e}}$ (follows from Eq. (7)) is by factor $R/2a$ greater than the previous estimate, equaling 0.973 and 1.886 for factors $f = 1.6$ and 3.1, respectively. The increase in the predicted ion flow at midplane position will then be a factor 2 or 2.9, depending on the chosen value of f.

Finally, for the JET probe position and the case of the combined flow, the ratio R is given by Eq. (7) with the angle $\alpha = 76°$, which is larger by factor 1/0.39 than previous estimates, and equaling 2.49 for $f = 1.6$ (only this value of f, related to JET experiments, should be used here). Hence, the maximum increase compared to the case of zero E_r can be of factor 3.5. This would completely remove the existing discrepancy between modelling and experiment on JET.

Summarising the above estimates, the following factors of increase in the simulated parallel ion flows could be expected provided experimentally measured E_r were obtained in the codes. For JET, assuming $f = 1.6$, and depending on whether only the Pfirsch-Schlüter or the combined ion flow is used, one expects factors 1.6 or 3.5 increase in the predicted ion flow. For AUG, assuming $f = 3.1$, and depending again on what model for the parallel ion flow is used, one expects factors 2.3 or 2.9 increase in the predicted ion flow. This is somewhat lower than the discrepancy of factor ~ 4 between measured and simulated peak Mach numbers of the parallel ion flow estimated in Section 4. However, as was pointed out in this section, this factor can be somewhat overestimated due to the probe position being vertically shifted with respect to the midplane position. For the JET case, a number of additional uncertainties comes from the fact that there is no direct correspondence between experimentally measured parameters and EDGE2D code results. For example, factor $f = 1.6$ used in the estimates of this section is an average value obtained from the statistical data representing large number of discharges. Further, for the calculation of the factors of increase of the code-predicted flow, formulas employing decay lengths taken for AUG plasmas (from Table 1) were used. Finally, even establishing the degree of inconsistency (estimated as being factor 3) between measured and predicted Mach numbers is subject to uncertainties, since experimental $\Delta M_{max}/2$ values lying in the range 0.25 – 0.34 were only very approximately compared with the corresponding modelling values varying from 0.08 for the high to 0.126 - for low density Ohmic cases.

7. Conclusions

Small values of radial electric field in the SOL predicted by 2D edge fluid codes EDGE2D and SOLPS can be the reason for large discrepancies between experimental and modelled Mach numbers of the parallel ion flow in the SOL. In the codes, the predicted E_r is close to zero, on average, while in the experiment it is found to be of order $-f\nabla T_e/e$, with factor f being above 1.5. This discrepancy is likely to be caused by the presence of supra-thermal electrons in the divertor [12]. Their presence is also believed to be responsible for the codes' underestimate of the target T_e [7,8]. The three known problems in the present-day code modelling: underestimate of the simulated target electron temperature T_e (so far, reliably established only at AUG), radial electric field E_r and parallel ion flows in the SOL, are likely to be related to each other and all caused by missing kinetic effects in electron parallel transport from the SOL to divertor that can't be modelled with the present-day fluid codes. Earlier reservations against the use of fluid equations (that assume strong collisionality) for parallel electron heat transport, based on the arguments about low collisionality of heat-carrying electrons, initiated the development of kinetic codes for the plasma edge modelling. Fluid codes continued to be widely used in parallel for modelling SOL and divertor plasmas in existing devices as well as for the prediction of divertor performance in ITER. The deficiency of fluid codes stemming from the incorrect treatment of the parallel heat transport was apparently masked by large uncertainties in some key boundary parameters, in particular, separatrix electron density, which is poorly defined in the experiment owing to an uncertainty in the determination of the separatrix position. The emerging experimental evidence of discrepancies between experiment and fluid code simulations calls into question the validity of fluid codes for SOL and divertor modelling.

Radial electric field, alongside ion pressure gradient, is one of the two drivers for the ion Pfirsch-Schlüter flow. Its correct simulation can therefore increase the predicted Mach number of the parallel ion flow. The Pfirsch-Schlüter flow, however, is not the only flow to be expected in the SOL. The 'return parallel flow', compensating poloidal E×B drift, was also identified both in the codes and experiment. The combined affect of the two flows, referred to as the 'combined flow' in the present paper, is expected to further increase the contribution of E_r to the parallel ion flow. At the outer midplane position, and using $f = 3.1$, obtained for the AUG standard Ohmic shot, an increase by factors 2.3 to 2.9 in the predicted Mach number, depending on whether one uses only the Pfirsch-Schlüter or the combined flow model, can be expected provided the codes simulated realistic values of E_r. This may still be somewhat insufficient to close the gap between SOLPS predicted and experimentally measured Mach numbers in AUG which is characterized by ~ factor 4 difference (however, this factor may be overestimated, see Sec. 6). For the position of the reciprocation probe in JET, and using $f = 1.6$, based on the data from large number of discharges, the factor of increase can vary from 1.6 to 3.5, depending on whether only the Pfirsch-Schlüter or the combined flow model is adopted. The latter factor of increase may entirely eliminate the difference, of order 3, between the experimentally determined part of the ion flow that depends on the toroidal field direction and the part of the modelled ion flow attributed to drifts.

References

[1] Erents S K, Pitts R A, Fundamenski W, Gunn J P and Matthews G F, Plasma Phys. Control. Fusion 46 (2004) 1753.

[2] Pitts R A, Andrew P, Bonnin X, et al., J.Nucl.Mater. 337-339 (2005) 146.

[3] Coster D P, Bonnin X, Chankin A, et al., 'Integrated modelling of material migration and target power handling at JET', in Fusion Energy 2004 (Proc. 20th Int. Conf. Vilamoura, 2004) (Vienna: IAEA) CD-ROM file TH/P5-18 and http://www-naweb.iaea.org/napc/physics/fec/fec2004/datasets/index.html.
[4] Müller H.W., Bobkov V., Rohde V., et al., proc. of 32nd EPS Conference on Plasma Phys. Tarragona, 27 June – 1 July 2005 ECA Vol.29C, P-1.009 (2005).
[5] Müller H.W., Bobkov V., Herrmann A., et al., 'Deuterium plasma flow in the scrape-off layer of ASDEX Upgrade', paper P3-15 presented at the 17th PSI Conference, Hefei, May 22-26 (2006), to be published in J. Nucl. Mater.
[6] Asakura N, Takenaga H, Sakurai S, et al., Nucl. Fusion 44 (2004) 503.
[7] Chankin A V, Coster D P, Dux R, et al., Plasma Phys. Control. Fusion 48 (2006) 1839.
[8] Chankin A V, Coster D P, Dux R, et al., 'Comparison between measured divertor parameters in ASDEX Upgrade and SOLPS code solutions', paper P1-40 presented at the 17th PSI Conference, Hefei, May 22-26 (2006), to be published in J. Nucl. Mater.
[9] Batishchev O V, Krasheninnikov S I, Catto Peter J, et al., Phys. Plasmas 4 (1997) 1672.
[10] Stangeby P C, in *The Boundary of Magnetic Fusion Devices*, IOP Publishing, Bristol (2000), p.658.
[11] Chankin A V, Coster D P, Dux R, et al, 'Critical issues identified by the comparison between experimental and SOLPS modelling on ASDEX Upgrade', in Fusion Energy 2004 (Proc. 20th Int. Conf. Chengdu, 2006) (Vienna: IAEA) CD-ROM file TH/P6-15 and http://www-naweb.iaea.org/napc/physics/fec/fec2006/html/index.htm.
[12] Chankin A V, Coster D P, Asakura N, et al., 'Discrepancy between modelled and measured radial electric fields in the scrape-off layer of divertor tokamaks: a challenge for 2D fluid codes ?', accepted for publication in Nuclear Fusion.
[13] Asakura N, Sakurai S, Shimada M, Koide Y, Hosogane N, and Itami K, Phys. Rev. Lett. 84 (2000) 3093.
[14] Pitts R A, Horacek H, Wischmeier M, 'Parallel SOL flow in TCV', paper O-16 presented at the 17th PSI Conference, Hefei, May 22-26 (2006), to be published in J. Nucl. Mater.
[15] Hutchinson I H, Phys. Fluids B 3 (1991) 847.
[16] Asakura N, and ITPA SOL and divertor topical group, 'Understanding the SOL flow in L-mode Plasma on divertor tokamaks, and its influence on the plasma transport', paper R-5 presented at the 17th PSI Conference, Hefei, May 22-26 (2006), to be published in J. Nucl. Mater.
[17] Keilhacker M, Daybelge U, Nucl. Fusion 21 (1981) 1497.
[18] LaBombard B, Lipschultz B, Nucl. Fusion 27 (1987) 81.
[19] Vershkov V A and the T-10 Group, the CIEP Group, J. Nucl. Mater. 162-164 (1989) 195.
[20] Pitts R A, Vayakis G and Matthews G F, J. Nucl. Mater. 176 & 177 (1990) 893.
[21] Fundamenski W. et al., 'Dissipative processes in interchange driven scrape-off layer turbulence', accepted for publication in Nuclear Fusion.
[22] Kirnev G S, Corrigan G, Coster D, Erents S K, Matthews G F, Pitts R A, J.Nucl. Mater. 337-339 (2005) 271.
[23] Groth M, Owen L W, Porter G D, et al., J. Nucl. Mater. 337-339 (2005) 425.
[24] Bonnin X, Coster D, Schneider R, Reiter D, Rozhansky V, Voskoboynikov S, J. Nucl. Mater. 337-339 (2005) 301.
[25] LaBombard B, Rice J E, Hubbard A E, et al., Nucl. Fusion 44 (2004) 1047.
[26] Tokar M Z, Kobayashi M, Feng Y, Physics of Plasmas 11 (2004) 4610.
[27] Kukushkin A S, Pacher H D, Plasma Phys. Control. Fusion 44 (2002) 931.
[28] Erents S K, Fundamenski W, Corrigan G, Matthews G F, Zagorski R, 'EDGE2D modelling of JET and ITER including the combined effect of Guiding Centre Drifts and an EDGE Transport Barrier', paper P3-6 presented at the 17th PSI Conference, Hefei,

May 22-26 (2006), to be published in J. Nucl. Mater.
[29] Hugill J, J. Nucl. Mater. 196-198 (1992) 918.
[30] Tendler M and Rozhansky V, Comments Plasma Phys. Control. Fusion 13 (1990) 191.
[31] Chankin A V, J. Nucl. Mater. 290-293 (2001) 518.
[32] Rozhansky V A, Voskoboynikov S P, Kaveeva E G, Coster D P and Schneider R, Nucl. Fusion 41 (2001) 387.
[33] MacLatchy C S, Boucher C, Poirier D A, Gunn J P, Stansfield B L, Zuzak W W, J. Nucl. Mater. 196-198 (1992) 248.
[34] Erents S K, Chankin A V, Matthews G F and Stangeby P C, Plasma Phys. Control. Fusion 42 (2000) 905.

Appendix A

In this appendix expressions for the velocity of the parallel ion flow in the 'main SOL', far away from the X-point and divertor, are derived. The particle source term due to the perpendicular (to the magnetic surfaces) transport is ignored. This source term is very important and is believed to be responsible for a large part of experimentally observed parallel ion flows related to the 'ballooning' nature of the perpendicular plasma transport. The focus of the present paper, however, is on the effects of classical quasi-steady-state drifts believed to be responsible for the changes in the parallel ion flow associated with the toroidal field reversal. The derivations of the present appendix extend the well-known formula for the velocity of the ion Pfirsch-Schlüter flow on the case of elliptical geometry and a possibility of the 'return parallel flow' in the SOL compensating poloidal E×B drift. Therefore, isothermal plasma with poloidally constant T_e and T_i, plasma electric potential and electron density, i.e. simplifying assumptions that led to the expression for the ion Pfirsch-Schlüter flow, will also be made here.

Ion poloidal particle flux is caused by perpendicular (within the flux surface, but perpendicular to the magnetic field, in the so called 'diamagnetic direction') diamagnetic and E×B drift velocities and the projection of the parallel velocity onto the poloidal plane:

$$nV_{i\theta}^{dr} = \left(\frac{\nabla p_i}{eB} - n\frac{E_r}{B} \right) \frac{B_\phi}{B}, \tag{A1}$$

$$nV_{i\theta}^{\parallel} = nV_{i\parallel} \frac{B_\theta}{B}, \tag{A2}$$

where B_ϕ, B_θ and B are toroidal, poloidal and total magnetic fields, and $\nabla p_i \equiv \partial p_i / \partial r$. In a steady-state, the combined ion flux must be divergence-free. By introducing Δ - small distance between neighbouring flux surfaces, this can be formulated as the requirement of zero poloidal gradient (s_θ - poloidal coordinate) of the total poloidal flow:

$$\frac{d}{ds_\theta}(nV_{i\theta}^{dr} \times 2\pi R\Delta + nV_{i\theta}^{\parallel} \times 2\pi R\Delta) = 0\,. \tag{A3}$$

Using $B_\theta R\Delta = const$, which is proportional to poloidal magnetic flux, and $n = const$, one obtains from the above equations:

$$\frac{d}{ds_\theta}\left(\frac{V_{i\theta}^{dr}}{B_\theta} + \frac{V_{i\parallel}}{B} \right) = 0\,. \tag{A4}$$

Below, a small difference between the full, B, and toroidal, B_ϕ, magnetic fields will be neglected as being second order in the small ratio B_θ/B. By introducing poloidally constant parameter $F_{dr} = \dfrac{V_{i\theta}^{dr} B}{B_\theta R}$ (owing to the fact that the poloidal dependence of $V_{i\theta}^{dr} \sim 1/B\Delta$, as follows from Eq. (A1), and $B_\theta R\Delta = const(\theta)$, the product proportional to poloidal magnetic flux), and using $B \sim 1/R$, Eq. (A4) can be cast into the shape:

$$\frac{d}{ds_\theta}(F_{dr}R^2 + V_{i\|}R) = 0\,, \tag{A5}$$

from where the solution for the ion parallel velocity easily follows:

$$V_{i\|} = -F_{dr}R + \frac{C}{R}\,, \tag{A6}$$

where C is a constant.

This equation gives the expression for parallel ion velocity in an arbitrary magnetic configuration, provided the constant of integration is known. The latter can either be determined from the knowledge of ion parallel velocity at some particular angle, or from some averaged value, such as *toroidal momentum* which is proportional to $\langle m_i n V_{i\|} / B_\theta \rangle$, where $\langle ... \rangle$ denotes averaging over the magnetic flux surface (remember that we consider constant n, and $1/B_\theta \sim R\Delta$). The latter generally involves numerical integration. However, for the case of zero toroidal momentum, elliptical plasmas and large aspect ratio, analytic solutions are easy to obtain. A circular case is no different from the elliptical one, so it will not be considered separately.

Zero toroidal momentum for the case of large aspect ratio $a/R = \varepsilon << 1$ implies that at the top and bottom of the magnetic configuration, where major radius coincides with that of the magnetic axis, $R = R_o$, ion parallel velocity is zero, hence, $C = F_{dr}R_o^2$. The solution for the ion parallel velocity is therefore given by:

$$V_{i\|} = -F_{dr}R_o\left(\frac{R}{R_o} - \frac{R_o}{R}\right). \tag{A7}$$

The ratio R/R_o for an ellipse is equal to:

$$\frac{R}{R_o} = 1 + \frac{a}{R_o}\left(1 + \frac{\tan^2\alpha}{k^2}\right)^{-1/2}. \tag{A8}$$

Neglecting terms quadratic in a/R_o, one obtains:

$$V_{i\|} = -F_{dr}R_o 2\frac{a}{R_o}\left(1 + \frac{\tan^2\alpha}{k^2}\right)^{-1/2}. \tag{A9}$$

Substituting F_{dr}, finally gives:

$$V_{i\|} = 2\frac{a}{R}\frac{B}{B_\theta}\left(\frac{E_r}{B} - \frac{\nabla p_i}{enB}\right)\left(1 + \frac{\tan^2\alpha}{k^2}\right)^{-1/2}, \tag{A10}$$

where k is ellipticity b/a.

For a cylindrical configuration, $k = 1$, $\left(1+\frac{\tan^2\alpha}{k^2}\right)^{-1/2} = \cos\alpha$ and the equation above has its usual Pfirsch-Schlüter form:

$$V_{i\|PS} = 2q\cos\alpha\left(\frac{E_r}{B} - \frac{\nabla p_i}{enB}\right), \tag{A11}$$

with $q = \frac{a}{R}\frac{B}{B_\theta}$ being safety factor.

Owing to $k > 1$, Eq. (A10) predicts somewhat larger parallel ion velocity compared to a cylindrical case, provided one uses the above (cylindrical) definition of q and poloidal angle α counted as shown in Fig. 1.

Instead of using zero velocity at the top and bottom of the machine, one could use an alternative boundary condition for parallel velocity at the entrance to the divertor corresponding to a situation where the transport effect of all poloidal E×B flow is compensated for by the creation of a *return parallel flow*. In this case the E_r should drop out of the contribution given by Eq. (A10) (since the E×B flow is completely compensated by the return parallel flow, and no non-divergence-free flows associated with E_r arise), and its contribution to the ion flow is fully accounted for by the inclusion of the return parallel flow velocity of E_r / B_θ. There is zero net transfer of plasma when $\frac{B_\theta}{B}\mathrm{v}_\|^{return} = \frac{B_\phi}{B}\frac{E_r}{B}$, i.e. approximately $\mathrm{v}_\|^{return} = \frac{E_r}{B_\theta}$. The expression for parallel ion velocity in this case can also be derived by specifying the boundary condition (with the second equality following from $E_{r_o}\Delta_o = E_r\Delta$ - potential difference between the flux surfaces, and $B_{\theta_o}\Delta_o R_o = B_\theta \Delta R$ - product proportional to poloidal magnetic flux):

$$V_{i\|}\Big|_{R=R_o} = \frac{E_{r_o}}{B_{\theta_o}} = \frac{E_r}{B_\theta}\frac{R_o}{R}, \tag{A12}$$

from where the constant of integration C can be found as:

$$C = \frac{E_r}{B_\theta}\frac{R_o^2}{R} + F_{dr}R_o^2. \tag{A13}$$

Substituting this constant into Eq. (A6) gives:

$$V_{i\|} = F_{dr}\left(\frac{R_o^2}{R} - R\right) + \frac{E_r}{B_\theta}\frac{R_o^2}{R^2}, \tag{A14}$$

leading to:

$$V_{i\|} = \frac{E_r}{B_\theta} - 2\frac{a}{R}\frac{B}{B_\theta}\frac{\nabla p_i}{enB}\left(1 + \frac{\tan^2\alpha}{k^2}\right)^{-1/2}. \tag{A15}$$